Molecular Basis of Resistance to HIV-1 Protease Inhibition: A Plausible Hypothesis†

Irene Luque, Matthew J. Todd, Javier Gómez, Nora Semo, and Ernesto Freire*

Department of Biology and Biocalorimetry Center, The Johns Hopkins University, Baltimore, Maryland 21218

Received February 2, 1998; Revised Manuscript Received March 6, 1998

ABSTRACT: The binding thermodynamics of the HIV-1 protease inhibitor acetyl pepstatin and the substrate Val-Ser-Gln-Asn-Tyr-Pro-Ile-Val-Gln, corresponding to one of the cleavage sites in the gag, gag−pol polyproteins, have been measured by direct microcalorimetric analysis. The results indicate that the binding of the peptide substrate or peptide inhibitor is entropically driven; i.e., it is characterized by an unfavorable enthalpy and a favorable entropy change, in agreement with a structure-based thermodynamic analysis based upon an empirical parameterization of the energetics. Dissection of the binding enthalpy indicates that the intrinsic interactions are favorable and that the unfavorable enthalpy originates from the energy cost of rearranging the flap region in the protease molecule. In addition, the binding is coupled to a negative heat capacity change. The dominant binding force is the increase in solvent entropy that accompanies the burial of a significant hydrophobic surface. Comparison of the binding energetics obtained for the substrate with that obtained for synthetic nonpeptide inhibitors indicates that the major difference is in the magnitude of the conformational entropy change. In solution, the peptide substrate has a higher flexibility than the synthetic inhibitors and therefore suffers a higher conformational entropy loss upon binding. This higher entropy loss accounts for the lower binding affinity of the substrate. On the other hand, due to its higher flexibility, the peptide substrate is more amenable to adapt to backbone rearrangements or subtle conformational changes induced by mutations in the protease. The synthetic inhibitors are less flexible, and their capacity to adapt is more restricted. The expected result is a more pronounced effect of mutations on the binding affinity of the synthetic inhibitors. On the basis of the thermodynamic differences in the mode of binding of substrate and synthetic inhibitors, it appears that a key factor to undertanding resistance is given by the relative balance of the different forces that contribute to the binding free energy and, in particular, the balance between conformational and solvation entropy.

The HIV-1 protease has been the most important target for drug development against HIV-1 infection due to its key role in viral maturation. The crystallographic structures of the free enzyme and the enzyme bound to several inhibitors have been determined at high resolution (see, for example, refs *1*−*6*). Several HIV-1 protease inhibitors are already in clinical use and have shown significant promise in combination therapies that include nucleoside inhibitors or multiple protease inhibitors. A serious clinical outcome has been the emergence of viral strains that exhibit resistance to multiple HIV-1 protease inhibitors (*7*−*10*). Loss of sensitivity to protease inhibitors occurs because the resistant viral strains encode for protease molecules containing specific amino acid mutations that lower the affinity for the inhibitors, yet maintain sufficient affinity for the substrate. The origins of the resistance are still unclear. While some of the observed mutations are located directly in the binding site, other mutations are at distal sites. It is also apparent that different inhibitors elicit different mutational patterns and that the patterns of cross resistance are not the same, despite the fact that all inhibitors target the same binding site.

The development of a new generation of protease inhibitors that effectively addresses the issue of resistance will require a better understanding of the interactions between protease and inhibitors, and between protease and substrates. In principle, resistance to an inhibitor can be acquired either by a preferential reduction of the binding affinity toward that inhibitor or by an enhanced catalytic activity that partially overcomes the inhibitor effect. It appears that for most of the mutants studied the catalytic activities of mutant proteases remain approximately constant and comparable to that of the wild-type protease, while the binding affinity toward inhibitors decreases significantly (*4*, *11*, *12*).

For some mutations, the affinity toward the inhibitor decreases by up to 3 orders of magnitude while the K_m for the substrate only changes by less than 1 order of magnitude (*4*, *11*, *12*). It can be hypothesized that, in those cases, resistance is due to the dissimilarities between substrate/protease and inhibitor/protease interactions. In principle, binding dissimilarities can be attributed to two different factors: (1) some of the protease residues critical for inhibitor binding are not critical for substrate binding and/or 2) the

† Supported by National Institutes of Health Grants GM57144, GM51362, and RR04328. I.L. is a visiting student from the Universidad de Granada, Granada, Spain, partially supported by a fellowship from the Ministerio de Educación y Ciencia (PB93-1163).

* To whom correspondence should be addressed. Phone: (410) 516-7743. Fax: (410) 516-6469. E-mail: bcc@biocal2.bio.jhu.edu.

S0006-2960(98)00252-9 CCC: $15.00 © 1998 American Chemical Society
Published on Web 04/11/1998

thermodynamic nature of the interactions is not the same, even if the same protease residues are involved in the binding of substrate and inhibitor.

In a previous paper, we examined the binding thermodynamics of 13 synthetic HIV-1 protease inhibitors for which high-resolution structures are available (*13*). In this paper we have studied the binding of substrates and inhibitors by a combination of thermodynamic measurements and structure-based calculations. Comparison of the binding characteristics of inhibitors and substrates has provided the necessary elements to advance a hypothesis for the molecular origin of resistance.

EXPERIMENTAL PROCEDURES

Enzyme Preparation. HIV-1 protease (mutant Q7K/L33I/L63I in *Escherichia coli* 1458) was kindly provided by Dr. A. G. Tomasselli (*14*). Cells were grown in Luria broth with 100 μg/mL ampicillin (25 °C). Protease was induced by temperature increase (40 °C), harvested by centrifugation after 4 h, and stored at −80 °C. Protease from washed inclusion bodies was solubilized in 50% HOAc and purified by gel-filtration chromatography (150 mL, Superdex-75, Pharmacia) in 50% HOAc and 0.3 M NH_4OAc at 4 °C as described (*15*). Purified mutant protease was stored either as lyophilized protein or in 50% HOAc. Protease was folded by rapid dilution into 30 volumes of assay buffer (100 mM NaOAc, pH 5.0, 1 mM EDTA, 1 mM DTT, 0.05% reduced Triton X-100) and then assayed directly or concentrated using ultrafiltration (Centriprep-10, Amicon) for calorimetric analysis. Protein used for calorimetric analysis was folded in the absence of detergent to prevent accumulation of detergent during ultrafiltration. Protease concentration was determined spectrophotometrically using an extinction coefficient $E_{1\%}$ of 11.8 at 280 nm (*16*).

Spectrophotometric Enzymatic Assays. Protease hydrolytic activity toward the chromogenic substrate [Lys-Ala-Arg-Val-Nle-nPhe-Glu-Ala-Nle-NH_2, California Peptide Research, Inc. (*17*)], with a purity better than 99.3% as determined by HPLC, was measured by monitoring the relative decrease in absorbance at 300 nm using an HP 8452A diode array spectrophotometer (Hewlett-Packard) and corrected for spectrophotometer drift (average absorbance at 296−304 nm minus 446−454 nm). A typical assay (120 μL in a 1 cm microcuvette) was initiated by adding protease (final concentration, 100 nM) into the assay buffer containing various concentrations of substrate. Hydrolysis rates were obtained from the initial rate data when less than 20% of substrate was hydrolyzed. Experiments were performed at different temperatures ranging from 15 to 35 °C.

Isothermal Titration Calorimetry. Isothermal titration calorimetry experiments were carried out using a MCS titration instrument (Microcal Inc., Northhampton, MA). In a typical calorimetric experiment, the enzyme solution in the calorimetric cell was titrated with the inhibitor solution. The heat evolved after each ligand injection was obtained from the integral of the calorimetric signal. To correct for heat effects not directly related to the binding reaction (primarily dilution of the ligand), control experiments were performed by making identical injections of the inhibitor solution into the calorimetric cell containing only buffer. The heat due to the binding reaction between the inhibitor and the enzyme was obtained as the difference between the heat of reaction and the corresponding heat of dilution. Analysis of the data was performed using software developed in this laboratory as described previously (*18*).

Calorimetric Assay of Enzymatic Activity. The calorimetric assays and data analysis were performed by following the method developed by Gomez et al. (*19*). This method is summarized here for the benefit of the reader. Substrate (Val-Ser-Gln-Asn-Tyr-Pro-Ile-Val-Gln from QCB, Hopkinton, MA, with a purity better than 99% by HPLC analysis) was dissolved in the assay buffer and allowed to achieve thermal equilibrium in the reaction cell of the titration calorimeter (1.4 mL). Hydrolysis was initiated by injecting a small volume of protease into the reaction cell (∼20 μL). The measured rate of heat change is directly proportional to the velocity of the enzymatic reaction $\partial Q/\partial t = -\Delta H V \partial[S]/\partial t$, where ΔH is the characteristic enthalpy of the reaction and V the volume of the reaction cell. ΔH is determined by allowing the reaction to proceed to completion and then dividing the integrated total heat by the amount of substrate depleted or product formed. The rate of substrate depletion ($-\partial[S]/\partial t$) is given by the standard equation:

$$-\frac{\partial[S]}{\partial t} = \frac{k_{cat}[E_0][S]_t}{K_m + [S]_t}$$

where $[E_0]$ is the enzyme concentration, $[S]_t$ is the substrate concentration at time t, k_{cat} is the catalytic constant, and K_m is the Michaelis constant. The possibility of competitive product inhibition was considered by making the apparent K_m a function of the amount of product formed at any time t; i.e., $K_{m,app} = K_m(1 + [P]_t/K_i)$, where $[P]_t = [S]_{t=0} - [S]_t$ is the concentration of product formed at time t and K_i is the product inhibition constant. Other possibilities such as linear noncompetitive inhibition or linear uncompetitive inhibition can be examined by modifying the above equation as described by Hyland et al. (*20*). Analysis of the data was performed by nonlinear least-squares fitting of the data to the above equation using software developed in this laboratory. Using this technique, the activity of protease toward both chromogenic and nonchromogenic substrates could be determined.

RESULTS AND DISCUSSION

Energetics of Peptide Inhibitor Binding. The energetics of the association of acetyl pepstatin (Ac-Val-Val-Sta-Ala-Sta) was measured by isothermal titration calorimetry. Figure 1 (panel A) shows a typical calorimetric titration of the HIV-1 protease at 25 °C. The calorimetric binding isotherm was obtained by plotting the integrated heat obtained after each injection versus the concentration of added inhibitor (Figure 1, panel B). Under the conditions of these experiments, each calorimetric titration provides the binding affinity, the Gibbs energy of binding, and the enthalpy and entropy changes. Analysis of the titration data yields a Gibbs energy of binding of -8.0 ± 0.2 kcal/mol and a binding enthalpy of 7 ± 0.5 kcal/mol. This result indicates that the binding of acetyl pepstatin is not favored enthalpically and that the favorable Gibbs energy of binding originates from a large positive entropy. Similar results have been obtained by Xie et al. (*21*) for pepstatin A at pH 6.5.

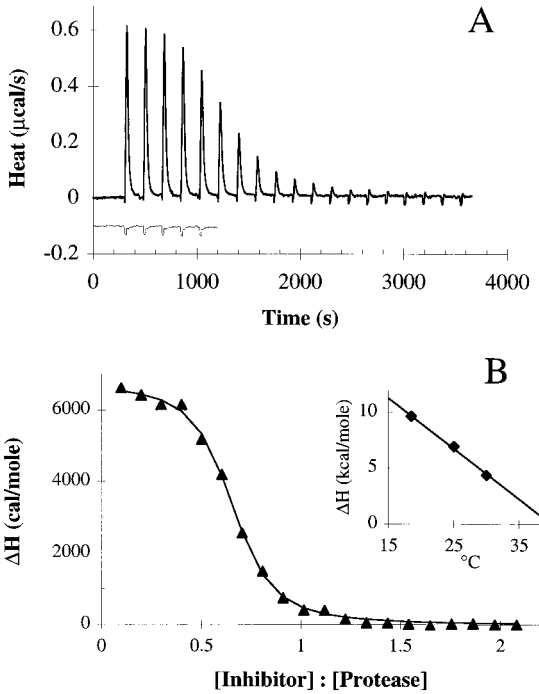

FIGURE 1: Calorimetric titration of HIV-1 protease with the peptide inhibitor acetyl pepstatin (Ac-Val-Val-Sta-Ala-Sta). Panel A shows the heat effects associated with the injection of acetyl pepstatin (10 μL per injection of a 280 μM solution) into the calorimetric cell (1.4 mL) containing HIV-1 protease at a concentration of 20 μM. The experiment was performed at 25 °C. Panel B shows the binding isotherm corresponding to the data in panel A and the best fitted curve. The inset in panel B shows the temperature dependence of the binding enthalpy. All experiments were performed in 20 mM sodium acetate and 0.2 mM EDTA, pH 5.5. Linear least-squares fit of the data yields a heat capacity change of −452 cal/(K·mol) for the binding of acetyl pepstatin.

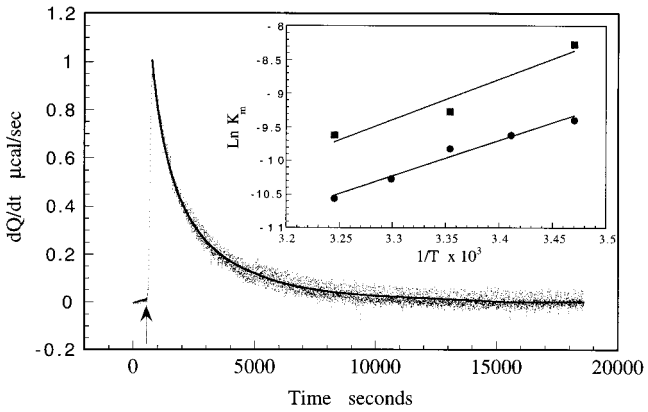

FIGURE 2: Direct monitoring of HIV-1 protease activity by isothermal titration calorimetry. The calorimetric trace was obtained at 25 °C after addition of a small volume (20 μL) of a solution containing HIV-1 protease ([E] = 0.89 μM) to the calorimetric reaction cell (1.4 mL) containing the nonapeptide substrate ([$S_{initial}$] = 750 μM). The solid line represents the best fit to the experimental data. Inset: Temperature dependence of the K_m for the nonapeptide substrate (closed circles) and the chromogenic substrate (closed squares). The van't Hoff plot in the figure (Ln K_m versus $1/T$) is consistent with binding enthalpies of 10.5 and 12 kcal/mol, respectively. The data for the chromogenic substrate were obtained spectrophotometrically.

At 25 °C the entropy change is equal to 50.3 cal/(K·mol), which amounts to a contribution to ΔG of −14.9 kcal/mol. Additional experiments performed in the temperature interval 18−40 °C were used to determine the temperature dependence of ΔH (inset in Figure 1B). These experiments were consistent with a ΔC_p of −452 cal/(K·mol). The thermodynamic parameters associated with this binding reaction are the characteristic signatures of a binding process driven by the gain in solvent entropy associated with the burial of a large hydrophobic surface.

Energetics of Substrate Binding. Isothermal reaction calorimetry allows measurement of enzymatic reactions by following in real time the rate of heat released or absorbed as a result of the hydrolysis of the substrate (*22*). Because the calorimetric observable is the heat associated with the reaction, the calorimetric assay can be performed directly on natural substrates without the need to introduce bulky chromogenic groups that may perturb the system under study. The peptide Val-Ser-Gln-Asn-Tyr-Pro-Ile-Val-Gln corresponds to one of the cleavage sites in the gag, gag−pol polyproteins (*23*). The HIV-1 protease cleaves the peptide bond between Tyr 5 and Pro 6 in the nonapeptide, positions commonly referred to as P1 and P1′ (*23*). Figure 2 shows the time course of the nonapeptide substrate hydrolysis as detected calorimetrically. In this figure, the measured rate of heat change ($\partial Q/\partial t$) has been plotted as a function of time. The data were analyzed as described in Experimental Procedures. The K_m value for the experiment in Figure 2 was 54 ± 10 μM, and the product inhibition constant, K_i, was of the same magnitude (∼60 μM). Dunn et al. (*23*) have previously estimated the K_m of this peptide as 150 μM at 37 °C, which is close to the value obtained calorimetrically. On the other hand, the binding affinity of hydrolysis products by the HIV-1 protease has been found to be of the same order of magnitude as the K_m for the substrate (*20*).

Calorimetric experiments such as the one shown in Figure 2 were performed at different temperatures between 15 and 35 °C in order to determine the enthalpy of binding (ΔH) of the substrate to the protease molecule (Figure 2, inset). It is clear that the binding affinity increases with temperature, as expected for a reaction characterized by a positive enthalpy of binding. Linear least-squares analysis of the data (Ln K_m vs $1/T$) are consistent with an enthalpy for association of 10.5 kcal/mol. As shown for acetyl pepstatin, this result indicates that the binding of the substrate is not favored enthalpically and that the favorable Gibbs energy of binding originates from a large positive entropy. At 25 °C the entropy change is equal to 54.7 cal/(K·mol), which amounts to a contribution to ΔG of −16.3 kcal/mol. Similar results were obtained using a standard spectrophotometric assay with the chromogenic substrate Lys-Ala-Arg-Val-Nle-nPhe-Glu-Ala-Nle-NH_2 (where nPhe denotes *p*-nitrophenylalanine and Nle, norleucine) (Figure 2, inset). In this case a positive binding enthalpy of 12 kcal/mol was obtained, indicating that the binding of this substrate is also entropically driven.

Structural Energetics of Acetyl Pepstatin Binding. The crystal structure of the complex between acetyl pepstatin and the HIV-1 protease has been solved at 2.0 Å resolution (*24*) (PDB file 5hvp). In this structure the inhibitor is found in two different orientations; therefore, the two conformations were used separately in structure-based thermodynamic calculations. For the free enzyme, the structure determined by Spinelli et al. (*1*) (PDB file 1hhp) was used. In the complex file (5hvp) the complete coordinates for the side

Table 1: Structure-Based Thermodynamic Analysis of Peptide Substrate and Inhibitor Binding to HIV-1 Protease[a]

	acetyl pepstatin (av)[b]	synthetic inhibitors (av)[c]	nonapeptide substrate I[d]	nonapeptide substrate II[d]
ΔC_p [cal/(K·mol)]	-427 ± 8 (-452)	-340 ± 50	-455	-489
$\Delta H(25)$ (cal/mol)	10050 ± 1550 (7000)	9050 ± 3000	9000 (10500)	11380 (10500)
ΔS_{conf} [cal/(K·mol)]	-36.95 ± 1.0	-19 ± 7	-67.3	-65.2
ΔS_{solv} [cal/(K·mol)]	123.8 ± 1.1	100 ± 12	139.3	147.1
ΔS_{other} [cal/(K·mol)]	-25.1 ± 0.1	-9.6 ± 0.7	-24.0	-23.4
ΔS_{total} [cal/(K·mol)]	61.75 ± 1.1 (50.3)	71.4 ± 12	48.0 (54.74)	58.5 (54.74)
$\Delta G(25)$ (cal/mol)	-8400 ± 930 (-8000)	-12250 ± 1360 (-11983 ± 2000)	-5315 (-5822)	-6050 (-5822)

[a] Structure-based thermodynamic calculations were performed as described previously (*25*−*30*). For acetyl pepstatin and substrate, the numbers in parentheses are the values measured experimentally herein. For the synthetic inhibitors the number in parentheses is the average experimental ΔG for the 13 inhibitors tabulated by Bardi et al. (*13*). [b] The results for acetyl pepstatin are the average for the two orientations and side chain conformations reported in the crystallographic structure (*24*). [c] The results for the synthetic inhibitors correspond to the 13 cases published by Bardi et al. (*13*). [d] In case I the structure of the complex between HIV-1 protease and the substrate was built by using the PDB file 4hvp as a template. In case II the PDB file 7hvp was used as a template. See text for details.

chains of Arg 41, Lys 43, Gln 61, and Ile 72 are not included. Those side chains were truncated at the same locations in the free enzyme file (1hhp). Also, Asn 37 was mutated to Ser in 5hvp. These amino acids are at exposed locations away from the binding site. These changes are implemented every time there are amino acid differences or differences in the number of atoms in the structures of the free and bound proteins. All calculations were performed as described before, using the structural parameterization of the binding energetics developed previously in this laboratory (*25*−*30*). All calculations were performed at a nominal pH of 5.5 assuming the coupling of the binding reaction to the protonation of one group with a pK_a of 3.5 (*20*, *31*).

Table 1 summarizes the results of the structure-based thermodynamic analysis for acetyl pepstatin. The calculations reproduce the experimental ΔG, ΔH, and ΔC_p values reasonably well, indicating that the structural parameterization effectively captures the magnitude and the balance of forces that determine the binding affinity. According to these results, the driving force for binding is the entropy gain associated with the release of solvent molecules upon burial of a predominantly hydrophobic surface. This favorable interaction is opposed by (1) the negative change in conformational entropy (peptide inhibitor plus protease side chains in binding pocket), (2) the negative change in translational entropy, and (3) a positive enthalpy change.

Structural Energetics of Natural Substrate Binding. The structure of the complex between protease and substrate was modeled using as a starting point the structure of the protease with the substrate-based inhibitor Ace-Thr-Ile-Nle═Nle-Gln-Arg-NH_2 (where ═ denotes a reduced peptide bond) (*5*) (PDB file 4hvp). This structure was used as a template to generate the structure of the nonapeptide substrate (Val-Ser-Gln-Asn-Tyr-Pro-Ile-Val-Gln) by mutating and adding the necessary residues and identifying the most probable conformation according to the Gibbs potential function derived from the structural parameterization (*32*). The building process was begun by positioning the central dipeptide Tyr-Pro containing the cleavage site in the binding pocket. The nonapeptide was built by adding the remaining amino acids using the backbone of the inhibitor as a guide. This procedure has been used before in the design of mutants of the peptide inhibitor pepstatin A (*32*). To verify the results, the structure of the complex between protease and substrate was also modeled using the structure of the protease with a substrate-based hydroxyethylamine inhibitor, Ac-Ser-Leu-Asn-Phe-ψ[CH(OH)CH_2N]-Pro-Ile-Val-OMe (*33*) (PDB file 7hvp). The results were similar in both cases, as shown in Table 1.

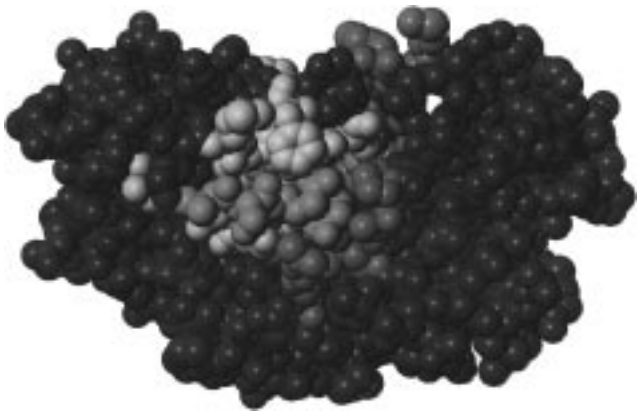

FIGURE 3: Predicted structural arrangement of the nonapeptide substrate in the binding pocket of the HIV-1 protease. The substrate is shown in red. Shown in yellow (subunit A) and green (subunit B) are the protease residues expected to contribute the most to the binding energetics.

The analysis of the predicted structure is consistent with a binding ΔG of -5.7 ± 0.4 kcal/mol at 25 °C, pH 5.5. The predicted ΔC_p is -472 ± 16 cal/(K·mol) and the predicted generic contribution to ΔH is 10.2 ± 1.2 kcal/mol at 25 °C, which are close to the experimental values (Table 1). The predicted ΔG is consistent with a binding affinity of 68 μM, which compares well with the experimental K_m value of 54 μM measured calorimetrically and the value of 150 μM reported earlier (*23*). In agreement with the experimental results, the thermodynamic analysis indicates that the binding of the substrate is not enthalpically favored and that the favorable contributions to the binding Gibbs energy are of an entropic origin. Analysis of the structural distribution of ΔH indicates that the enthalpy change due to the substrate/protease interactions per se is favorable (~ -3 kcal/mol) and that the unfavorable binding enthalpy arises from the rearrangement of the flap region in each subunit upon binding. This rearrangement involves primarily residues 40−60 corresponding to the flap itself and residues 60−84 corresponding to the immediately adjacent β strand. A similar situation is observed with the binding of the peptide inhibitor acetyl pepstatin.

The theoretical structure of the complex between the HIV-1 protease and the natural substrate is shown in Figure 3. Highlighted in this figure are the protease residues that are predicted to contribute more than 0.15 kcal/mol to the

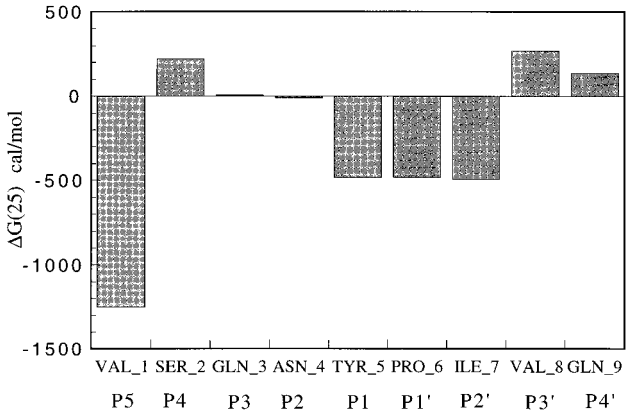

FIGURE 4: Generic contributions of each residue in the nonapeptide substrate to the Gibbs energy of binding. As shown, the largest contribution to ΔG is made by Val 1, followed by Tyr 5, Pro 6, and Ile 7. These results indicate that in the natural substrate the residues directly at the cleavage site P1, P1′, and P2′ and that at position P5 contribute the most to the binding energetics.

generic Gibbs energy of binding. The theoretical structure suggests strong van der Waals contacts between the protease and the substrate. These contacts are particularly strong in the region near Val 1, which corresponds to the P5 position which is relatively distal from the cleavage site. These interactions contribute favorably to the binding enthalpy.

In Figure 4, the calculated structural map for the generic contributions of the natural substrate to the Gibbs energy of binding shows that the largest contribution to ΔG is made by Val 1, followed by Tyr 5, Pro 6, and Ile 7. Surprisingly, the remaining residues contribute very little to the Gibbs energy of binding. Analysis of the entire map (not shown) indicates that most of the binding energy is contributed by the protease molecule itself rather than the substrate. The predicted large contribution of Val 1 is consistent with the experimental observation that the K_m for the shorter peptide substrate lacking Val 1 and Gln 9 is close to 1 order of magnitude weaker (*23*). According to our calculations the bulk of the difference is given by the absence of Val 1. The experimental observation that the nature of the residues at position P3 (Gln 3 in the natural peptide) is relatively unimportant (*23*) is consistent with the lack of a significant contribution to ΔG by this residue. The situation is similar with substitutions at the P2 position (Asn 4 in the natural peptide). The conclusions of this analysis emphasize the role of residues at distant positions (e.g., P5 position, Val 1 in the natural peptide) from the cleavage site as previously noted by Dunn et al. (*23*, *34*).

Structural Mapping of Peptide Substrate and Inhibitor Binding. Previously, we presented an analysis of 13 synthetic protease inhibitors (A77003, A78791, A76928, A74704, A76889, VX478, SB203386, SB203238, SB206343, U100313, U89360, A98881, CGP53820) (*13*). These inhibitors are substrate analogues designed to compete with natural substrates for the same binding site and therefore are expected to interact with the same set of residues in the protease molecule. The structural distribution of the protease interactions with inhibitors and substrate is summarized in Figure 5. The contributions listed include only contact contributions made by individual residues in the protease molecule. It is evident that the same protease residues contribute to the binding energetics of both inhibitor and substrate, albeit with different magnitudes. This result suggests that the origin of resistance resides in the thermodynamic partitioning of the interaction energetics rather than the identity of the residues that interact with the inhibitors or substrate.

Fundamental Differences between Peptide Substrate and Inhibitor Binding. For the 13 synthetic inhibitors considered in the analysis, the intrinsic enthalpy of binding is also predicted to be unfavorable, with values ranging between 1.3 and 12.2 kcal/mol (*13*). The only synthetic inhibitor measured calorimetrically (SB203386), albeit with the SIV protease, yielded a binding enthalpy of 6.4 kcal/mol (*35*), which is within the expected range. These enthalpy values are similar in magnitude to those measured for the substrate and also for acetyl pepstatin (Table 1). In all cases the

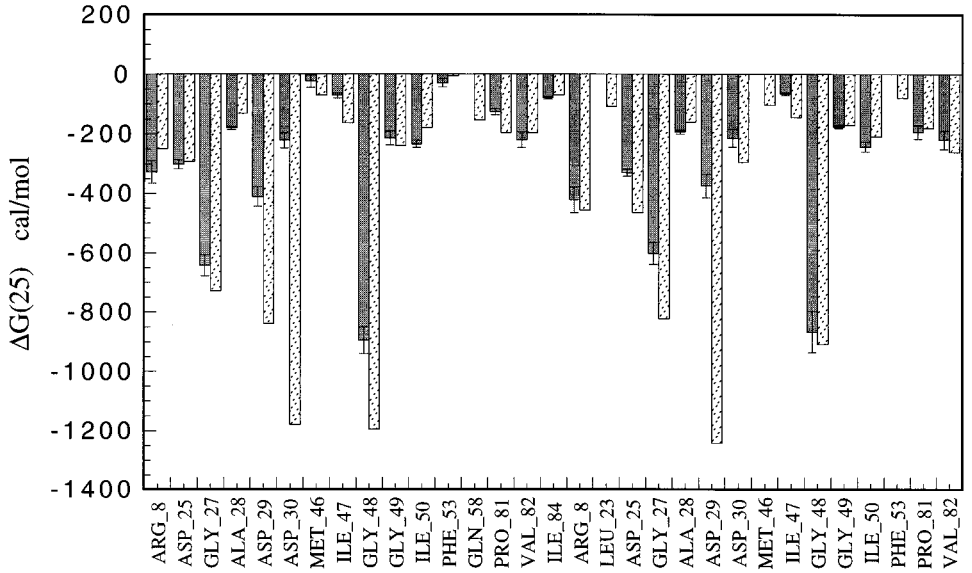

FIGURE 5: Comparison of the intrinsic contributions of HIV-1 protease residues to the Gibbs energy of binding to synthetic inhibitors (A77003, A78791, A76928, A74704, A76889, VX478, SB203386, SB203238, SB206343, U100313, U89360, A98881, CGP53820) (dark bars) and to the nonapeptide substrate Val-Ser-Gln-Asn-Tyr-Pro-Ile-Val-Gln (light bars). For the 13 synthetic inhibitors the bars denote the average contributions and the error bars denote the standard deviation.

binding enthalpy is unfavorable; however, the binding affinity of the synthetic inhibitors is in the nanomolar range while that of the substrates is in the micromolar range. Inhibitors and substrates overcome the unfavorable binding enthalpy by a favorable entropy change. The major contributions to the entropy change are the solvation and conformational entropies, which are of opposite signs (Table 1). The favorable entropy change is due to the gain in solvent entropy that originates from the burial of a large hydrophobic surface upon binding. This favorable gain in solvent entropy is opposed by the loss of conformational and translational entropy. The peptide substrate has a high flexibility in solution, and when it binds to the protease, it loses a significant number of degrees of freedom. The synthetic inhibitors, on the other hand, are small organic molecules with fewer degrees of freedom in solution and therefore lose fewer degrees of freedom upon binding. For the 13 synthetic inhibitors, the conformational entropy change averages −19 ± 7 cal/(K·mol) (*13*) (Table 1). The binding of the nonapeptide substrate, on the other hand, involves a conformational entropy change of −67 cal/(K·mol). Overall, the synthetic inhibitors end up with a higher binding affinity due to their higher rigidity in solution.

The above results suggest a possible explanation for the molecular origin of resistance. Due to their higher flexibility, peptide substrates are more amenable to adapt to backbone rearrangements or subtle conformational changes induced by mutations in the protease. On the other hand, more rigid molecules have fewer degrees of freedom, and their capacity to adapt is more restricted. The result is that the peptide substrate is able to maintain strong contacts with a mutant protease whereas the synthetic inhibitors are less able to accommodate to a geometrically distorted binding pocket. In general, inhibitors with low flexibility will exhibit a higher specificity toward a selected target but will lose their high affinity, even with minor changes in the geometry of the binding site. The higher specificity of the synthetic inhibitors is due in part to their conformational rigidity. As a corollary, more flexible molecules will generally show lower specificity. For example, the peptide inhibitor acetyl pepstatin has a higher conformational flexibility, and consequently, its binding affinity for HIV-1 protease mutants decreases much less than the affinity of a synthetic inhibitor. In addition, we note that acetyl pepstatin inhibits a larger number of aspartic proteases.

The hypothesis advanced above is supported by the existing structural information for resistant mutants. For example, it has been shown by Baldwin et al. (*12*) that the effect of the resistant mutant V82A cannot be rationalized in terms of the deletion of a single methyl group in each chain of the protease. Analysis of the crystallographic structure of the resistant mutant revealed a widespread rearrangement of the backbone around the binding pocket (*12*). The structure-based thermodynamic analysis indicates that the Gibbs free energy of binding is redistributed throughout the entire binding pocket (*13*). Analogous results have been obtained for the binding of mutants V82D and V82N with the inhibitor U-89360E (*4*). In both cases the loss in binding affinity by the synthetic inhibitors can be rationalized in terms of their inability to successfully accommodate to a distorted binding pocket.

Thus, on the basis of the thermodynamic differences observed between substrate and inhibitors, it appears that a key factor to understanding resistance is the relative balance of enthalpic and entropic contributions to the Gibbs energy of binding, in particular, the role of conformational entropy in determining the binding affinity. Within this thermodynamic framework, specificity and resistance become the two sides of the same coin.

ACKNOWLEDGMENT

We thank Dr. John Louis and Dr. Dong Xie for many helpful discussions.

REFERENCES

1. Spinelli, S., Liu, Q. Z., Alzari, P. M., Hirel, P. H., and Poljak, R. J. (1991) *Biochimie 73*, 1391−1396.
2. Wlodawer, A., and Erickson, J. W. (1993) *Annu. Rev. Biochem. 62*, 543−585.
3. Kim, E. E., Baker, C. T., Dwyer, M. D., Murcko, M. A., Rao, B. G., Tung, R. D., and Navia, M. A. (1995) *J. Am. Chem. Soc. 117*, 1181−1182.
4. Hong, L., Treharne, A., Hartsuck, J. A., Foundling, S., and Tang, J. (1996) *Biochemistry 35*, 10627−10633.
5. Miller, M., Schneider, J., Sathyanarayana, B. K., Toth, M. V., Marshall, G. R., Clawson, L., Selk, L., Kent, S. B. H., and Wlodawer, A. (1989) *Science 246*, 1149−1153.
6. Abdel-Meguid, S. S., Metcalf, B. W., Carr, T. J., Demarsh, P., DesJarlais, R. L., Fisher, S., Green, D. W., Ivanoff, L., Lambert, D. M., Murthy, K. H. M., Petteway, J. S. R., Pitts, W. J., Tomaszek, J. T. A., Winborne, E., Baoguang Zhao, B., Dreyer, G. B., and Meek, T. D. (1994) *Biochemistry 33*, 11671−11677.
7. Kaplan, A. H., Michael, S. F., Wehbie, R. S., Knigge, M. F., Paul, D. A., Everitt, L., Kempf, D. J., Norbeck, D. W., and Erickson, J. W. (1994) *Proc. Natl. Acad. Sci. U.S.A. 91*, 5597−5601.
8. Ho, D. D., Toyoshima, T., Mo, H., Kempf, D. J., Norbeck, D., Chen, C., Wideburg, N. E., Burt, S. K., Erickson, J. W., and Singh, M. K. (1994) *J. Virol. 68*, 2016−2020.
9. Condra, J. H., Schleif, W. A., Blahy, O. M., Gabryelski, L. J., Graham, D. J., Quintero, J. C., Rhodes, A., Robbins, H. L., Roth, E., Shivaprakash, M., Titus, D., Yang, T., Teppler, H., Squires, K. E., Deutsch, P. J., and Emini, E. A. (1995) *Nature 374*, 569−571.
10. Roberts, N. A. (1995) *AIDS 9*, S27−S32.
11. Lin, Y., Lin, X., Hong, L., Foundling, S., Heinrikson, R. L., Thaisrivongs, S., Leelamanit, W., Raterman, D., Shah, M., Dunn, B. D., and Tang, J. (1995) *Biochemistry 34*, 1143−1152.
12. Baldwin, E. T., Bhat, T. N., Liu, B., Pattabiraman, N., and Erickson, J. W. (1995) *Nat. Struct. Biol. 2*, 244−249.
13. Bardi, J. S., Luque, I., and Freire, E. (1997) *Biochemistry 36*, 6588−6596.
14. Mildner, A. M., Rothrock, D. J., Leone, J. W., Bannow, C. A., Lull, J. M., Reardon, I. M., Sarcich, J. L., Howe, W. J., Tomich, C. C., Smith, C. W., Heinrickson, R. L., and Tomasselli, A. G. (1994) *Biochemistry 33*, 9405−9413.
15. Hui, J. O., Tomasselli, A. G., Reardon, I. M., Lull, J. M., Brunner, D. P., Tomich, C.-S. C., and Heinrikson, R. L. (1993) *J. Protein Chem. 12*, 323−327.
16. Polgar, L., Szeltner, Z., and Boros, I. (1994) *Biochemistry 33*, 9351−9357.
17. Richards, A. D., Phylip, L. H., Farmerie, W. G., Scarborough, P. E., Alvarez, A., Dunn, B. M., Hirel, P.-H., Konvalinka, J., Strop, P., Pavlickova, L., Kostka, V., and Kay, J. (1990) *J. Biol. Chem. 265*, 7733−7736.
18. Freire, E., Mayorga, O. L., and Straume, M. (1990) *Anal. Chem. 62*, 950A−959A.
19. Gomez, J., Todd, M. J., and Freire, E. (1998) manuscript in preparation.

20. Hyland, L. J., Tomaszek, T. A., Roberts, G. D., Carr, S. A., Magaard, V. W., Bryan, H. L., Fakhoury, S. A., Moore, M. L., Minnich, M. D., Culp, J. S., DesJarlais, R. L., and Meek, T. D. (1991) *Biochemistry 30*, 8441−8453.
21. Xie, D., Gulnik, S., Collins, L., Gustchina, E., Bhat, T. N., and Erickson, J. W. (1997) in *Structure and function of aspartic proteinases: Retroviral and cellular enzymes* (James, M., Ed.) Plenum, New York (in press).
22. Morin, P., and Freire, E. (1991) *Biochemistry 30*, 8494−8500.
23. Dunn, B. M., Gustchina, A., Wlodawer, A., and Kay, J. (1994) *Methods Enzymol. 241*, 254−285.
24. Fitzgerald, P. M. D., McKeever, B. M., Van Middlesworth, J. F., Springer, J. P., Heimbach, J. C., Leu, C.-T., Herber, W. K., Dixon, R. A. F., and Darke, P. L. (1990) *J. Biol. Chem. 265*, 14209−14218.
25. Murphy, K. P., and Freire, E. (1992) *Adv. Protein Chem. 43*, 313−361.
26. Gomez, J., Hilser, J. V., Xie, D., and Freire, E. (1995) *Proteins: Struct., Funct., Genet. 22*, 404−412.
27. Hilser, V. J., Gomez, J., and Freire, E. (1996) *Proteins 26*, 123−133.
28. Lee, K. H., Xie, D., Freire, E., and Amzel, L. M. (1994) *Proteins. Struct. Func. and Genetics 20*, 68−84.
29. DAquino, J. A., Gómez, J., Hilser, V. J., Lee, K. H., Amzel, L. M., and Freire, E. (1996) *Proteins 25*, 143−156.
30. Luque, I., Mayorga, O., and Freire, E. (1996) *Biochemistry 35*, 13681−13688.
31. Hyland, L. J., Tomaszek, J. T. A., and Meek, T. D. (1991) *Biochemistry 30*, 8454−8463.
32. Luque, I., Gomez, J., Semo, N., and Freire, E. (1998) *Proteins 30*, 74−85.
33. Swain, A. L., Miller, M. M., Green, J., Rich, D. H., Schneider, J., Kent, S. B. H., and Wlodawer, A. (1990) *Proc. Natl. Acad. Sci. U.S.A. 90*, 8805−8809.
34. Griffiths, J. T., Phylip, L. H., Konvalinka, J., Strop, P., Gustchina, A., Wlodawer, A., Davenport, R. J., Briggs, R., Dunn, B. M., and Kay, J. (1992) *Biochemistry 31*, 5193−5200.
35. Hoog, S. S., Towler, E. M., Zhao, B., Doyle, M. L., Debouck, C., and Abdel-Meguid, S. S. (1996) *Biochemistry 35*, 10279−10286.

BI9802521